IEEE Access
Multidisciplinary ⋮ Rapid Review ⋮ Open Access Journal

Received 13 September 2023, accepted 30 September 2023, date of publication 4 October 2023,
date of current version 11 October 2023.

Digital Object Identifier 10.1109/ACCESS.2023.3321892

RESEARCH ARTICLE

Adaptive Hybrid Compensation Control of Inertia Uncertainty and Disturbance for Variable Structure Hypersonic Vehicle

KAI-YU HU[1,2], YUQING CHENG[2], AND CHUNXIA YANG[2]
[1]College of Automation Engineering, Nanjing University of Aeronautics and Astronautics, Nanjing 211106, China
[2]304th Institution, China Aerospace Science and Industry Corporation, Beijing 100074, China

Corresponding author: Kai-Yu Hu (hkywuyue@163.com)

This work was supported in part by the National Natural Science Foundation of China under Grant 61922042 and Grant 61873127.

ABSTRACT This paper presents an adaptive hybrid compensation scheme for disturbances and uncertain inertia parameters of variable-structure hypersonic flight vehicles (HFV). A nominal nonlinear dynamic inverse (NDI) controller with variable-structure harmonic functions guarantees that the system outputs precisely follow the reference commands for a longitudinal HFV model with modelling errors. In the case of inertia uncertainty, a multi-learning law-adaptive NDI controller is proposed to directly compensate for its influence on the tracking performance, which makes the variable-structure HFV robust to inertia uncertainty and reduces the high vibration of velocity and attitude angles. Subsequently, an improved adaptive variable structure NDI controller with a sliding-mode disturbance observer is designed to actively compensate for sea-skimming disturbances and continuously ensure anti-disturbance flight quality. Finally, the active-passive hybrid adaptive control algorithms compensate for the inertia uncertainty and disturbance of the variable-structure HFV. The proposed method's efficacy was verified through a semi-physical system simulation, while Lyapunov functions demonstrated the system stability.

INDEX TERMS Hybrid compensation, hypersonic flight vehicle, disturbance observer, dynamic inverse.

I. INTRODUCTION

The high manoeuvring sea skimming technology of variable-structure hypersonic vehicles (HFV) is becoming the core technology for missiles because it can effectively avoid detection and interception [1], [2], [3]. However, deformation, steering, and sea-skimming cruise at speeds above Mach 5 pose challenges to the controller [4], [5]. The main control problems include modelling errors or unmodeled dynamics caused by strong nonlinearity, deformation, parameter uncertainty caused by variable structure manoeuvring, sudden airflow, and complex disturbances caused by sea water vapor wave at the sea surface [6], [7], [8]. Owing to the real-time requirement, variable-structure HFV cannot over-rely on the observer but must ensure the pertinence and accuracy of compensation. Therefore, a hybrid scheme combining passive direct compensation and observer-based active compensation was designed in this study to realise the automatic repair of inertia uncertainty and disturbance simultaneously, ensuring the stable flight of a high-manoeuvrability variable-structure HFV.

In recent years, the HFV model has seen a rapid development of nonlinear control technologies. A full-state tracking error system was devised in [9] to tackle the unpredictability of parameters and the unmodeled dynamics, and a fuzzy logic system was used to detect the nonlinear system. In [10], to update the neural weights in an HFV, a nonlinear prediction error was used to construct a learning law. In [11], considering the actuator dynamics and asymmetric nonlinear constraints, a fuzzy adaptive design method was used to solve the finite-time constraint tracking problem of an HFV. Fuzzy logic was employed to linearise the nonlinear equation of the model in [12], and radial basis functions were used to approximate the external nonlinear disturbance, transforming

The associate editor coordinating the review of this manuscript and approving it for publication was Min Wang.

a classical HFV into another model. A nonlinear feedback design technique, driven by error, was suggested in [13] for a type of uncertain multi-input multi-output nonlinear systems with a specified tracking capability, in order to improve the dynamic performance of fuzzy adaptive dynamic surface control. The HFV fast response necessitated the employment of a series of harmonic functions to eradicate the nonlinear effects of variable structural parameters, while the nonlinear dynamic inverse (NDI) was utilized to directly protect against the modelling errors resulting from linearisation.

Owing to the widespread parameter uncertainty in HFV, there has been little progress in the research on relevant compensation strategies in recent years [14], [15], [16]. In [17], a parameterised tracking error model of an HFV was derived considering some uncertainties that were approximated by an interval Type II fuzzy neural network. In [18], smooth functions and linear time-varying models were introduced to estimate the boundary of time-varying uncertainty, effectively compensate for the influence of faults, and achieve stable altitude and velocity tracking. In [19], for an uncertain HFV model, fault and hysterical actuators were used for high-performance adaptive controls. In [20], a directed topology of a networked uncertain spacecraft was investigated to determine the finite-time attitude formation-containment control problem. Subsequently, in [21], an adaptive timing attitude stabilisation of a rigid spacecraft with inertial uncertainty, external disturbances, actuator saturation, and faults was examined. However, these methods rarely mention variable-structure systems and modelling errors, nor can they simultaneously deal with complex disturbances. This study addresses these limitations.

More advanced disturbance suppression technology enables HFV to accurately engage targets in high-mobility, sea-skimming flight, and electromagnetic countermeasures [22], [23], [24], [25]. In [26], an active disturbance rejection control scheme was proposed for the electromagnetic docking of spacecraft with time-varying delays, fault signals, external disturbances, and elliptic eccentricity. Proposals for two terminal sliding mode control strategies to address the finite-time attitude-tracking issue, with environmental interference and model uncertainty, were made in [27]. Thence a smooth input MRS model was suggested in [28], and incorporating backstepping and a finite-time perturbation observer, was devised to address the finite-time attitude-tracking issue in the face of environmental interference and model uncertainty. A rapid terminal sliding mode algorithm was employed in [29] to create a disturbance observer to calculate the uncertainty and disturbance, while guaranteeing that the estimation error converges to the origin. In [30], the worst Nash strategy was proposed for perturbations defined as players, and the authors rigorously proved that there was an open-loop Nash equilibrium in the problem. A nonlinear disturbance observer observed an uncertain system disturbance in [31] as a lumped, unknown term, and its effect was counterbalanced by a strong backstepping compensator. However, the above methods do not consider the inertia uncertainty of high-manoeuvrability sea skimming flights, which is an industry challenge that must be addressed. This study aims to solve this problem.

In recent years, in order to obtain stronger penetration and mixed martial arts ability, the variable structure design idea is gradually integrated into the control technology. In [32], a quasi-soft variable structure control system was designed, covering the discretization effects, permitted maintaining the favorable properties of fast convergence and smooth inputs. In [33], considering that the complexity of existing safety controls were determined by the geometrical properties of the environment, a variable structure control was proposed to isolate the environment's geometrical complexity from the control structure. A variable exponential reaching law based on position error and a saturation function was suggested in [34] as an adjustable structure controller for position tracking speed and chattering performance, in order to optimize both. In [35], a variable structure control approach was proposed for vehicles platooning based on a hierarchical fuzzy logic. In [36], a tolerant controller of a six-phase induction generator via a variable structure strategy was tested and compared with a classical proportional-integral controller. However, the above prior art do not take into account the special circumstances of HFV: the uncertainty caused by variable structure, the strong disturbance and parameter uncertainty caused by sea skimming, and the more complex uncertainty problems associated with variable structure parameter uncertainty. This paper will combine the existing variable structure methods with the engineering practice of the variable structure HFV.

In this paper, to solve the flight mode switching problem of variable-structure HFV, direct adaptive harmonic functions are designed based on known variable-structure parameters to eliminate the influence of variable-structure processes on stability. A passive-active hybrid compensation scheme is designed to deal with the inertial uncertainty and disturbance of a high-manoeuvring sea skimming flight. A direct passive compensation method is used to suppress the inertia uncertainty, and disturbance estimation and active sliding-mode NDI control are used to compensate for the disturbance. At last, the HFV of variable-structure stayed steady despite modelling blunder, parameter doubt, and disruption. The contributions of this study are as follows.

1) A kind of adaptive control parameter is designed which can change its own value along with the variable aerodynamic surface of the structure, then directly reconcile the nominal and variant flight states, so that both flight modes are stable.

2) A passive robust and observer-based disturbance rejection hybrid compensation scheme was designed to solve inertial uncertainty and disturbance problems. After the nominal variable-structure NDI controller shields the modelling errors of the linearised model, a composite adaptive variable-structure NDI algorithm is designed for the uncertain parameter of inertia, which does not rely on the observer to passively compensate for the uncertainty.

3) A disturbance observer of sliding mode was crafted to augment the compound adaptive variable structure NDI algorithm's purpose, allowing the active sliding mode variable structure algorithm to adjust for intricate elastic mode disturbances in accordance with the observed disturbance value.

This paper's rest is organized thus: Section II showcases the linearised HFV model with modelling errors and a nominal variable structure NDI controller. Section III proposes a hybrid compensation strategy, namely passive compensation of uncertain parameters and active compensation of disturbance. Verifying the proposed method's validity is the focus of Section IV. Section V then summarizes the study.

II. HFV MODEL AND NDI CONTROLLER

A NDI controller of nominal variable structure is crafted for the longitudinal variable structure HFV in this section. First, the non-variant classical HFV model is given, and then transformed into variable structure HFV model after adding relevant parameter. Finally, some harmonic functions with variable structural parameter is designed and added to the NDI controller to form a basic adaptive NDI algorithm. The following section will be able to address other control issues through the utilization of these designs.

A. LONGITUDINAL MODEL

The longitudinal HFV system with fixed structure has the following state equations:

$$\begin{cases} \dot{x} = Ax + Bu \\ y = Cx + Du \end{cases} \tag{1}$$

where x is the system state variable, u the system input, and y the system output. These satisfy the following requirements:

$$\begin{cases} x = [\alpha, q, \theta]^T \\ u = \delta_e \\ y = [\dot{\alpha}, \alpha, q, \theta, \dot{q}]^T \end{cases} \tag{2}$$

Referring to [2], the system states and input/output matrices A, B, C and D are expressed as (3)–(6), shown at the bottom of the page, where the compound state parameters of pneumatic and structural can be expressed as

$$Y^{\alpha} = \frac{P_0 \cos\frac{\alpha_0}{57.3} + 57.3C_{z,\alpha} \times 0.5\rho V^2 S}{mV} \tag{7}$$

$$Y^{\delta_e} = \frac{57.3C_{z,\delta_e} \times 0.5\rho V^2 S}{mV} \tag{8}$$

$$M_z^{\alpha} = \frac{57.3C_{m,\alpha} \times 0.5\rho V^2 Sb}{I_y} \tag{9}$$

$$M_z^{\delta_e} = \frac{57.3C_{m,\delta_e} \times 0.5\rho V^2 Sb}{I_y} \tag{10}$$

$$M_z^{\dot{\alpha}} = \frac{C_{m,\dot{\alpha}} \times 0.5\rho VSb^2}{I_y} \tag{11}$$

$$M_z^{q} = \frac{C_{m,q} \times 0.5\rho VSb^2}{I_y} \tag{12}$$

At the system equilibrium point, the linearization method should be employed; this is the state point of the dynamic system with a state vector change rate of 0 for HFV. The equilibrium point is the spot where the flight trajectory and attitude remain steady, such as horizontal flight, hover, climb, and other state points.

Remark 1: The system balance state is selected as follows: altitude $H = 0$ m, Mach $M = 15$Ma, equilibrium point flying

$$A = \begin{bmatrix} -Y^{\alpha} + \frac{g}{V_*}\sin\mu_* & 1 & -\frac{g}{V_*}\sin\mu_* \\ M_z^{\alpha} - M_z^{\dot{\alpha}}(Y^{\alpha} - \frac{g}{V_*}\sin\mu_*) & M_z^{q} + M_z^{\dot{\alpha}} & -M_z^{\dot{\alpha}}\frac{g}{V_*}\sin\mu_* \\ 0 & 1 & 0 \end{bmatrix} \tag{3}$$

$$B = \begin{bmatrix} -Y^{\delta_e} \\ M_z^{\delta_e} - M_z^{\dot{\alpha}}Y^{\delta_e} \\ 0 \end{bmatrix} \tag{4}$$

$$C = \begin{bmatrix} -Y^{\alpha} + \frac{g}{V_*}\sin\mu_* & 1 & -\frac{g}{V_*}\sin\mu_* \\ 1 & 0 & 0 \\ 0 & 1 & 0 \\ 0 & 0 & 1 \\ M_z^{\alpha} - M_z^{\dot{\alpha}}(Y^{\alpha} - \frac{g}{V_*}\sin\mu_*) & M_z^{q} + M_z^{\dot{\alpha}} & -M_z^{\dot{\alpha}}\frac{g}{V_*}\sin\mu_* \end{bmatrix} \tag{5}$$

$$D = \begin{bmatrix} -Y^{\delta_e} \\ 0 \\ 0 \\ 0 \\ M_z^{\delta_e} - M_z^{\dot{\alpha}}Y^{\delta_e} \end{bmatrix} \tag{6}$$

TABLE 1. Variable meaning table.

	Parameter meaning
$C_{z,\alpha}$	Attack angle lift coefficient
C_{z,δ_e}	Lift coefficient due to elevator angle
$C_{m,\alpha}$	Pitching moment coefficient due to attack angle
C_{m,δ_e}	Pitching moment coefficient due to elevator angle
$C_{m,\dot{\alpha}}$	Pitching moment coefficient due to attack angle rate
$C_{m,q}$	Pitch moment coefficient due to pitch rate
Y^{α}	Derivative of lift coefficient with respect to attack angle
Y^{δ_e}	Derivative of lift coefficient with respect to elevator angle
$M_{z\alpha}$	Longitudinal static stability derivative
$M_z^{\delta_e}$	Derivative of pitch moment coefficient to elevator angle
$M_z^{\dot{\alpha}}$	Derivative of pitch moment coefficient with respect to attack angle rate
M_{zq}	Derivative of pitch moment coefficient with respect to pitch rate

speed $V^* = 5104.41$ m/s, equilibrium point angle of attack $\alpha_0 = 3.25°$, equilibrium point ideal flight path inclination μ^*, ide and longitudinal aerodynamic surface air mass P_0 per unit time meet:

$$\begin{cases} \mu_{*,\text{ide}} = 0 \\ P_0 = 15.1\text{kg} \end{cases} \tag{13}$$

Set the air density equilibrium state to

$$\begin{cases} \rho_0 = 0.1249\text{kg} \cdot \text{s}^2/\text{m}^4 \\ \rho = \rho_0 g = 1.22\text{kg/m}^3 \\ g = 9.806\text{m/s}^2 \end{cases} \tag{14}$$

The longitudinal model of the equilibrium point is in an ideal state, and the modelling error is on the ideal orbital inclination μ^*, ide. The real variable structure system cannot completely guarantee that the equilibrium point orbital inclination μ^* is zero. Therefore, this study assumes that there is an unknown modelling error $\Delta\mu^*$, that satisfies:

$$|\Delta\mu_*| \le \mu_{\max} \le 5° \tag{15}$$

$$\mu_* = \mu_{*,ide} + \Delta\mu_* \tag{16}$$

At long last, model (1) is a HFV system that is vertically invariant, taking into account the modelling errors, where α is the attack angle, q is the pitch rate, θ is the pitch angle, $\dot{\alpha}$ is the attack angle derivative, $\dot{q}$ is the pitch rate derivative, $\dot{\theta}$ is the angle derivative, δ_e is the elevator deflection angle, $\mu*$ is the track inclination, $V*$ is the flight speed, m is the aircraft mass, S is the wing area, b is the Span, I_y is the pitch inertia. The implications for the remaining variables in this model are presented in Tables 1.

Remark 2: Modelling errors lead to nonlinearity of the state parameters, making system (1) nonlinear. The variable structure parameter strengthens this nonlinear characteristic; therefore, the controller must first meet the requirements of compound nonlinear control. In this study, a variable-structure NDI algorithm is designed to solve this problem.

The variable structure function of HFV is directly manifested as shape change, which will directly affect the aerodynamic area. Therefore, the function describing the variable structure amplitude is the known aerodynamic area perturbation ΔS. In this study, ΔS is defined as a smooth variable structure parameter satisfies

$$\begin{cases} -\Delta S_{max} \le \Delta S \le \Delta S_{max} \\ \Delta S_{max} > 0 \end{cases} \tag{17}$$

and based on this, the aerodynamic and structural parameters of variable structure HFV are reconstructed, (18)–(27) as shown at the bottom of the next page.

According to (24)∼(27) and (3)∼(6), the variable structure parameters A_{VS}, B_{VS}, C_{VS} and D_{VS} can be calculated. Finally, the HFV model with these variable structural parameters is constructed into the following form:

$$\begin{cases} \dot{x} = (A + A_{VS})x + (B + B_{VS})u \\ y = (C + C_{VS})x + (D + D_{VS})u \end{cases} \tag{28}$$

B. NOMINAL VARIABLE STRUCTURE NDI CONTROLLER

In order for the system state variable $x = [\alpha, q, \theta]^T$ to track the given command $x_c = [\alpha_c, q_c, \theta_c]^T$ during HFV flight, a nominal variable structure NDI controller must be designed according to Formula (1). When the HFV has no inertial uncertainty, the NDI controller is designed as follows:

$$u = (B + B_{VS})^{-1}[-(A + A_{VS})x + \upsilon] \tag{29}$$

where υ is the virtual controller satisfies:

$$\upsilon = \dot{x}_c - (K + K_{hvs})e \tag{30}$$

where

$$e = x - x_c \tag{31}$$

The feedback gain matrix, K, is typically (32) and its form is determined by the constant desired valuer of states $\dot{x}_c$, which is usually 0.

$$K = \begin{bmatrix} w_\alpha & 0 & 0 \\ 0 & w_q & 0 \\ 0 & 0 & w_\theta \end{bmatrix} \tag{32}$$

K_{hvs} is a harmonic function of self-regulation with variable structural parameters, which is designed as follows:

$$K_{hvs} = \begin{bmatrix} w_{11}\Delta S & 0 & 0 \\ 0 & w_{22}\Delta S & 0 \\ 0 & 0 & w_{33}\Delta S \end{bmatrix} \tag{33}$$

The bandwidths of the control loops, denoted by w_α, w_q, and w_θ, are 40rad/s, 0.6rad/s, and 40rad/s respectively. w_{11}, w_{22}, and w_{33} are the constants of proportionality to be designed. The results show that the larger the w_α and w_θ are, the more serious the oscillation of the response curves

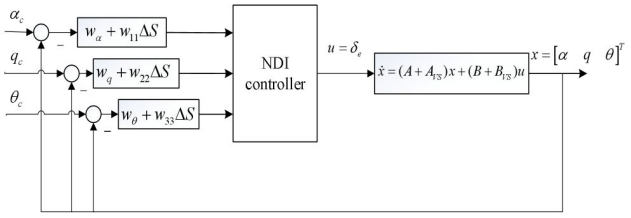

FIGURE 1. The nominal variable structure NDI scheme of the variable structure HFV.

are. The smaller the w_q, the more severe the oscillation of the response curves are. The block diagram of the nominal variable structure NDI controller is shown in Figure 1.

III. HYBRID COMPENSATION SCHEME

This section discusses the design of a variable-structure HFV adaptive NDI hybrid compensator with uncertain inertial parameters and disturbances to stabilise a closed-loop system. To achieve this control objective, the following issues were addressed in this study:

1) Contemplating the intricate longitudinal variable structure model, how to address the nonlinear inertial uncertainty parameters in the linearised system, and how to utilize the nonlinear control technique to create the adaptive control laws in the model.

2) Contemplating the intricate disturbance caused by sea skimming flight and elastic modes, in addition to the uncertainty of inertia parameters, how can one make up for both disturbances and uncertain parameters in the variable structure control scheme.

A. ADAPTIVE NDI CONTROLLER WITH INERTIAL UNCERTAINTY

Theoretically, the nominal variable-structure NDI controller (29) can enable HFV to track the given flight instructions. However, in an actual flight, the control channels are easily affected by the external flight environment, resulting in uncertainties in the aircraft parameters. In this study, the uncertainty of inertia was taken into account, and to enhance the flight control system's robustness, the moment of inertia was suppressed. The drift characteristics of the moment of

$$\Delta Y^{\alpha} = \frac{P_0 \cos\frac{\alpha_0}{57.3} + 57.3C_{z,\alpha} \times 0.5\rho V^2(S+\Delta S)}{mV} - Y^{\alpha} \tag{18}$$

$$\Delta Y^{\delta_e} = \frac{57.3C_{z,\delta_e} \times 0.5\rho V^2(S+\Delta S)}{mV} - Y^{\delta_e} \tag{19}$$

$$\Delta M_z^{\alpha} = \frac{57.3C_{m,\alpha} \times 0.5\rho V^2(S+\Delta S)b}{I_y + \Delta I_y} - M_z^{\alpha} \tag{20}$$

$$\Delta M_z^{\delta_e} = \frac{57.3C_{m,\delta_e} \times 0.5\rho V^2(S+\Delta S)b}{I_y + \Delta I_y} - M_z^{\delta_e} \tag{21}$$

$$\Delta M_z^{\dot{\alpha}} = \frac{C_{m,\dot{\alpha}} \times 0.5\rho V(S+\Delta S)b^2}{I_y + \Delta I_y} - M_z^{\dot{\alpha}} \tag{22}$$

$$\Delta M_z^{q} = \frac{C_{m,q} \times 0.5\rho V(S+\Delta S)b^2}{I_y + \Delta I_y} - M_z^{q} \tag{23}$$

$$A + A_{VS} = \begin{bmatrix} -(Y^{\alpha}+\Delta Y^{\alpha}) + \frac{g}{V_*}\sin\mu_* & 1 & -\frac{g}{V_*}\sin\mu_* \\ (M_z^{\alpha}+\Delta M_z^{\alpha}) - (M_z^{\dot{\alpha}}+\Delta M_z^{\dot{\alpha}})((Y^{\alpha}+\Delta Y^{\alpha}) - \frac{g}{V_*}\sin\mu_*) & M_z^{q}+\Delta M_z^{q}+M_z^{\dot{\alpha}}+\Delta M_z^{\dot{\alpha}} & -(M_z^{\dot{\alpha}}+\Delta M_z^{\dot{\alpha}})\frac{g}{V_*}\sin\mu_* \\ 0 & 1 & 0 \end{bmatrix} \tag{24}$$

$$C + C_{VS} = \begin{bmatrix} -(Y^{\alpha}+\Delta Y^{\alpha}) + \frac{g}{V_*}\sin\mu_* & 1 & -\frac{g}{V_*}\sin\mu_* \\ 1 & 0 & 0 \\ 0 & 1 & 0 \\ 0 & 0 & 1 \\ (M_z^{\alpha}+\Delta M_z^{\alpha}) - (M_z^{\dot{\alpha}}+\Delta M_z^{\dot{\alpha}})((Y^{\alpha}+\Delta Y^{\alpha}) - \frac{g}{V_*}\sin\mu_*) & M_z^{q}+\Delta M_z^{q}+M_z^{\dot{\alpha}}+\Delta M_z^{\dot{\alpha}} & -(M_z^{\dot{\alpha}}+\Delta M_z^{\dot{\alpha}})\frac{g}{V_*}\sin\mu_* \end{bmatrix} \tag{25}$$

$$B + B_{VS} = \begin{bmatrix} -Y^{\delta_e} - \Delta Y^{\delta_e} \\ M_z^{\delta_e} + \Delta M_z^{\delta_e} - (M_z^{\dot{\alpha}} + \Delta M_z^{\dot{\alpha}})(Y^{\delta_e} + \Delta Y^{\delta_e}) \\ 0 \end{bmatrix} \tag{26}$$

$$D + D_{VS} = \begin{bmatrix} -Y^{\delta_e} - \Delta Y^{\delta_e} \\ 0 \\ 0 \\ 0 \\ M_z^{\delta_e} + \Delta M_z^{\delta_e} - (M_z^{\dot{\alpha}} + \Delta M_z^{\dot{\alpha}})(Y^{\delta_e} + \Delta Y^{\delta_e}) \end{bmatrix} \tag{27}$$

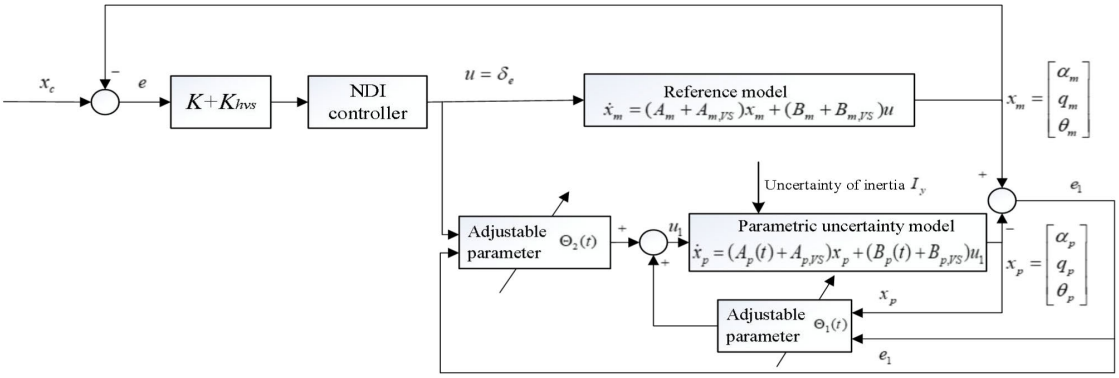

FIGURE 2. Adaptive NDI passively compensate diagram of the longitudinal variable structure HFV.

inertia parameter were modeled, and the uncertainty was expressed in a random fashion:

$$I_y = I_{y0}(1 + \Delta I_y) \tag{34}$$

The nominal value of parameter I_y, denoted by I_{y0}, is situated at the moment of inertia around the Y-axis. ΔI_y is the uncertain increment of parameter I_y, and its value range is

$$\begin{cases} -I_{y1} \le \Delta I_y \le I_{y1} \\ I_{y1} > 0 \end{cases} \tag{35}$$

I_{y1} is a positive constant.

To enhance the robustness of the system, a compound adaptive NDI controller based on a reference model was designed to directly and passively compensate for uncertain parameters. This renders the variable-structure HFV unaffected by the uncertainty of the inertia parameter moment, and the system outputs accurately track the given reference signals. A block diagram of the control scheme is presented in Figure 2.

The design process of this adaptive variable structure NDI controller is as follows:

Consider the system reference model, namely the indeterminate variable structure model, which is as follows:

$$\dot{x}_m = (A_m + A_{m,VS})x_m + (B_m + B_{m,VS})u \tag{36}$$

The actual system model with moment of inertia uncertainty is as follows:

$$\dot{x}_p = (A_p(t) + A_{p,VS})x_p + (B_p(t) + B_{p,VS})u \tag{37}$$

According to the reference model, the nominal variable structure NDI controller (see Section II-B) is designed as follows:

$$u = g^{-1}(x)[\dot{x}_c - (K + K_{hvs})e] \tag{38}$$

where $e = x - x_c$, K is the control bandwidth matrix, and K_{hvs} is the variable structure adaptive harmonic function.

The generalized error vector of the system is

$$e_1 = x_m - x_p \tag{39}$$

The equation using the generalized error as the state vector is

$$\begin{aligned}\dot{e}_1 = {} & A_m e_1 + [A_m + A_{m,VS} - A_p(t) - A_{p,VS} - (B_p(t) \\ & + B_{p,VS})\Theta_1(t)]x_p + [B_m + B_{m,VS} - (B_p(t) \\ & + B_{p,VS})\Theta_2(t)]u\end{aligned} \tag{40}$$

In order to make the uncertain system (37) respond to input u the same as the dynamic response of the reference model (36) to input u, the adaptive laws adjust $\Theta_1(t)$ and $\Theta_2(t)$ so that the uncertain system model matches the reference model, i.e

$$\begin{aligned} A_m + A_{m,VS} &= A_p(t) + A_{p,VS} + (B_p(t) + B_{p,VS})\Theta_1^* \\ &= A_p(t) + A_{p,VS} + B_p(t)\Theta_1^* + B_{p,VS}\Theta_1^* \end{aligned} \tag{41}$$

$$\begin{aligned} B_m + B_{m,VS} &= (B_p(t) + B_{p,VS})\Theta_2^* \\ &= B_p(t)\Theta_2^* + B_{p,VS}\Theta_2^* \end{aligned} \tag{42}$$

The function with '$*$' represents the optimal state when the model is perfectly matched, and Equation (36) can be expressed as

$$\begin{aligned}\dot{e}_1 = {} & (A_m + A_{m,VS})e_1 + (B_m + B_{m,VS})\Theta_2^{*-1}\tilde{\Theta}_1 x_p + (B_m \\ & + B_{m,VS})\Theta_2^{*-1}\tilde{\Theta}_2 u\end{aligned} \tag{43}$$

The errors of the two adjustable functions are 1×3 matrix and 1×1 matrix respectively satisfy

$$\tilde{\Theta}_1 = \Theta_1^* - \Theta_1 \tag{44}$$

$$\tilde{\Theta}_2 = \Theta_2{}^* - \Theta_2 \tag{45}$$

Theorem 1: For a generalised error system (40), there exists a Lyapunov function that contains state error e_1 and tunable function errors (44) and (45). If there exist adjustable parameters P, R_1, R_2, $R_{1,h\ vs}$, and $R_{2,h\ vs}$ such that the derivative of the Lyapunov function satisfying the condition is less than zero, system (40) is stable.

Proof: Using Lyapunov theory to design the adaptive law, as follows:

$$V = \frac{1}{2}e_1^T Pe_1 + \frac{1}{2}tr[\tilde{\Theta}_1^T(R_1 + R_{1,hvs})^{-1}\tilde{\Theta}_1^T] + \frac{1}{2}tr(\tilde{\Theta}_2^T(R_2 + R_{2,hvs})^{-1}\tilde{\Theta}_2^T) \tag{46}$$

where $tr(\cdot)$ represents the trace of matrix, that is, the sum of diagonal elements. By taking the derivative of the Lyapunov function, we obtain

$$\begin{aligned}\dot{V} = &\frac{1}{2}e_1^T[P(A_m + A_{m,VS}) + (A_m + A_{m,VS})^T P]e_1 \\ &+tr[\dot{\tilde{\Theta}}_1^T(R_1+R_{1,hvs})^{-1}\tilde{\Theta}_1^T + x_p e_1^T P(B_m+B_{m,VS})\Theta_2^{*-1}\tilde{\Theta}_1] \\ &+tr(\dot{\tilde{\Theta}}_2^T(R_2+R_{2,hvs})^{-1}\tilde{\Theta}_2^T + ue_1^T P(B_m+B_{m,VS})\Theta_2^{*-1}\tilde{\Theta}_2) \\ \le &\ 0\end{aligned} \tag{47}$$

where $P \in R^{3\times3}, R_1 \in R^{3\times3}, R_2 \in R, R_{1,h\ vs} \in R^{3\times3}$, and $R_{2,h\ vs} \in R$ are the positive definite symmetric matrices, we take

$$\begin{cases} P = diag(15, 2, 0) \\ R_1 = diag\ (0.5, 0.5, 0.5) \\ R_2 = 20 \\ R_{1,hvs} = diag(15, 15, 15) \\ R_{2,hvs} = 20 \end{cases} \tag{48}$$

When debugging the parameters, the larger R_1 and $R_{1,hvs}$ are, the smaller the system oscillation, but the slower the response speed; the larger R_2 and $R_{2,h\ vs}$ are, the faster the system responds, but the oscillation also increases.

If (46) is true, then the following conditions must be satisfied:

$$(A_m + A_{m,VS})^T P + P(A_m + A_{m,VS}) < 0 \tag{49}$$

To ensure that (47) is negative-definite, the second and third terms should always be zero, therefore

$$\begin{aligned}\dot{\tilde{\Theta}}_1 &= -(R_1 + R_{1,hvs})[(B_m + B_{m,VS})\Theta_2^{*-1}]Pe_1x_p^T \\ &= (-R_1 - R_{1,hvs})(B_m + B_{m,VS})\Theta_2^{*-1}Pe_1x_p^T\end{aligned} \tag{50}$$

$$\begin{aligned}\dot{\tilde{\Theta}}_2 &= -(R_2 + R_{2,hvs})[(B_m + B_{m,VS})\Theta_2^{*-1}]Pe_1u^T \\ &= (-R_2 - R_{2,hvs})(B_m + B_{m,VS})\Theta_2^{*-1}Pe_1u^T\end{aligned} \tag{51}$$

where the errors of the adjustable parameters are

$$\begin{cases} \tilde{\Theta}_1 = \Theta_1^* - \Theta_1 \\ \tilde{\Theta}_2 = \Theta_2{}^* - \Theta_2 \end{cases} \tag{52}$$

The design of the adaptive parameter updating laws are as follows:

$$\dot{\Theta}_1 = (R_1 + R_{1,hvs})(B_m + B_{m,VS})\Theta_2^{*-1}Pe_1x_p^T \tag{53}$$

$$\dot{\Theta}_2 = (R_2 + R_{2,hvs})(B_m + B_{m,VS})\Theta_2^{*-1}Pe_1u^T \tag{54}$$

$$\Theta_1(t) = \int_0^t (R_1+R_{1,hvs})(B_m+B_{m,VS})\Theta_2^{*-1}Pe_1x_p^T dt + \Theta_1(0) \tag{55}$$

$$\Theta_2(t) = \int_0^t (R_2+R_{2,hvs})(B_m+B_{m,VS})\Theta_2^{*-1}Pe_1u^T dt + \Theta_2(0) \tag{56}$$

Theorem 1 is proven based on inequality (49) and the laws of adaptation. Finally, the general variable-structure system in (40) is stable. □

Remark 3: When designing the algorithm, $R_{1,h\ vs}$ and $R_{2,h\ vs}$ shall be set according to the definition domain of variable structure parameter ΔS. They can be the functions that change with ΔS, or they can be a set of fixed values to ensure that the bounded variable structure process does not change the stability at any change in the domain.

In conclusion, when inertial uncertainty occurs, the passive adaptive variable-structure NDI controller with multiple adaptive laws can directly compensate for the inertial uncertainty and maintain a stable variable-structure HFV flight.

B. ACTIVE SLIDING MODE NDI CONTROLLER FOR DISTURBANCE

To optimise the above compound adaptive variable-structure NDI with passive compensation inertia uncertainty, a sliding mode scheme is added to improve the NDI controller to actively compensate for the influence of disturbances on the HFV. This improved measure can help HFV adapt to complex disturbances during sea skimming flights. The nonlinear model of the variable-structure HFV under disturbance can be expressed as

$$\begin{cases} \dot{x} = (A + A_{VS})x + (B + B_{VS})u + d \\ y = (C + C_{VS})x + (D + D_{VS})u \end{cases} \tag{57}$$

where $d(t)$ represents an external uncertainty disturbance. According to the corresponding cancellation principle in NDI, the controller of the nonlinear system is designed for the simultaneous existence of disturbance and inertia uncertainty, as follows:

$$u_* = (B + B_{VS})^+[-(A + A_{VS})x + \upsilon - d] \tag{58}$$

Therefore, control u obtained by ignoring the disturbance solution in the previous section is an ideal flight controller. As skimming becomes increasingly higher and closer to the sea surface, the ever-present $d(t)$ will increase, and the system will slowly diverge and become unstable. A slidingmode disturbance observer is employed to calculate the disturbance value, d is substituted by $\hat{d}$ for (58) and the active compensation control law is then employed to rectify the issue.

Figure 3 displays a block diagram of the variable-structure NDI in its active sliding-mode.

A sliding-mode variable structure system, with a variable structure observer, is constructed for a nonlinear, uncertain system having multiple inputs and outputs (57):

$$\begin{cases} s = x - z \\ \dot{z} = (B + B_{VS})u - \upsilon \\ \hat{d} = -[\upsilon + (A + A_{VS})x] \end{cases} \tag{59}$$

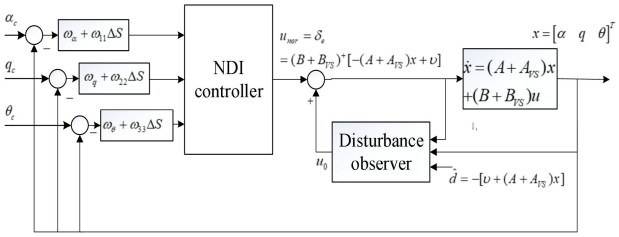

FIGURE 3. Active sliding mode variable structure NDI controller.

The auxiliary sliding mode surface is accompanied by the sliding mode virtual variable, denoted as $s = [s_1, s_2, s_3]^T$.

$$\begin{aligned} \upsilon &= [\,\upsilon_1 \quad \upsilon_2 \quad \upsilon_3\,]^T \\ &= -(\phi + \phi_{hvs})sign(s) \\ &= -\phi sign(s) - \phi_{hvs} sign(s) \end{aligned} \tag{60}$$

and

$$sign(s) = [sign(s_1) \quad sign(s_2) \quad sign(s_3)]^T \tag{61}$$

$$\phi = diag(\phi_1, \phi_2, \phi_3) \tag{62}$$

$$\phi_{hvs} = diag(\phi_{1,hvs}, \phi_{2,hvs}, \phi_{3,hvs}) \tag{63}$$

The variable structure harmonic function ϕ_{hvs} satisfies:

$$\begin{cases} \phi_{1,hvs} = k_1 \Delta S \\ \phi_{2,hvs} = k_2 \Delta S \\ \phi_{3,hvs} = k_3 \Delta S \end{cases} \tag{64}$$

and $k_1, k_2, k_3 \in R$ are constant. v can be expressed as (65), $i = 1, 2, 3$,

$$\begin{aligned} \upsilon_i &= -(\phi_i + \phi_{i,hvs})sign(s_i) \\ &= -\phi_i sign(s_i) - \phi_{i,hvs} sign(s_i) \end{aligned} \tag{65}$$

$$\upsilon = \left[\, -\upsilon_1 sign(s_1) \quad -\upsilon_2 sign(s_2) \quad -\upsilon_3 sign(s_3)\,\right]^T \tag{66}$$

Let

$$\xi = (A + A_{VS})x + \hat{d} = [\xi_1 \quad \xi_2 \quad \xi_3]^T \tag{67}$$

when $\phi_i + \phi_{i,h\,vs} > |\xi_i|$, the disturbance observation converges uniformly to the truth value $\hat{d}$.

Take the derivative of the first formula of (60) as:

$$\begin{aligned} \dot{s} &= \dot{x} - \dot{z} \\ &= (A + A_{VS})x + (B + B_{VS})u + d - (B + B_{VS})u + \upsilon \\ &= (A + A_{VS})x + d + \upsilon \end{aligned} \tag{68}$$

Theorem 2: A sliding-mode dynamic system (60) is uniformly stable when algorithms (61)∼(66) designed for system (60) satisfy condition (69).

$$\begin{cases} \upsilon_i = -\phi_i sign(s_i) - \phi_{i,hvs} sign(s_i) \\ \phi_i + \phi_{i,hvs} > |\xi_i| \end{cases} \tag{69}$$

Proof: Take the following Lyapunov function as

$$V = \frac{1}{2} s^T s \geq 0 \tag{70}$$

thence

$$\begin{aligned} \dot{V} &= s^T \dot{s} \\ &= \sum_{i=1}^{3} s_i \dot{s}_i \\ &= \sum_{i=1}^{3} s_i (\xi_i + \upsilon_i) \end{aligned} \tag{71}$$

Define

$$\dot{V}_i = s_i(\xi_i + \upsilon_i) \tag{72}$$

Because (69), we obtain

$$\begin{aligned} \dot{V}_i &= s_i(\xi_i + \upsilon_i) \\ &= s_i\xi_i - s_i(\phi_i + \phi_{i,hvs})sign(s_i) \\ &\leq s_i|\xi_i| - s_i(\phi_i + \phi_{i,hvs})sign(s_i) \\ &< s_i(\phi_i + \phi_{i,hvs}) - s_i(\phi_i + \phi_{i,hvs})sign(s_i) \\ &= \begin{cases} 0, s_i \geq 0 \\ 2s_i\phi_i < 0, s_i < 0 \end{cases} \end{aligned} \tag{73}$$

And then (74) can be obtained as

$$\begin{cases} \dot{V}_i < 0 \\ \dot{V} = \sum_{i=1}^{3} \dot{V}_i < 0 \end{cases} \tag{74}$$

Consequently, s is secure at the source, and meets the stability criterion. □

When the system reaches a stable point, it can be seen from equations (57)∼ (59) that the observed disturbance value is

$$\hat{d} = -[\upsilon + (A + A_{VS})x] \tag{75}$$

The simulation process's tracking performance is affected by the large amount of chattering caused by v being a switching function; thus, the relatively smooth hyperbolic tangent function tanh(s) can be employed to reduce this chattering, instead of the switching function sign(s)

Variable structure disturbance compensation law is designed as

$$u_o = -(B + B_{VS})^+ \hat{d} \tag{76}$$

Finally, the adaptive sliding-mode variable-structure NDI controller with passive direct compensation for the inertia uncertainty and active compensation for the disturbance (hybrid compensation) is as follows:

$$\begin{aligned} u_* &= u_{nor} + u_o \\ &= (B + B_{VS})^+[-(A + A_{VS})x + \upsilon] - (B + B_{VS})^+ \hat{d} \\ &= (B + B_{VS})^+[\upsilon - (A + A_{VS})x - \hat{d}] \end{aligned} \tag{77}$$

The Figure 4 block diagram of the adaptive sliding mode variable structure NDI controller is a result of the combination of adaptive and sliding mode control.

Remark 4: As shown in Figure 4, when disturbance occurs, the observer's estimated disturbance value is

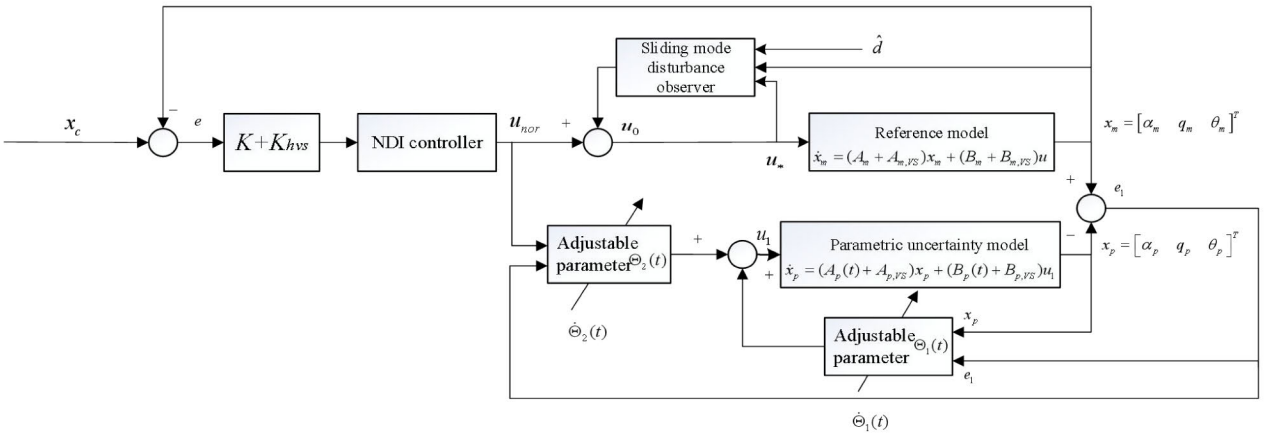

FIGURE 4. General diagram of adaptive sliding mode NDI control for longitudinal HFV model.

transmitted to the controller, and the controller directly cancels out the actual disturbance with NDI. When the HFV performs variable structure maneuvering flight, the controller immediately receives the variable structure parameters from the HFV integrated controller and directly reconstructs the control algorithm with these parameters, so that the HFV can quickly adapt to the variable structure mode. Experiments will verify the flight stability of the proposed scheme under harsh and multi-mode conditions.

Remark 5: In the composite guidance system, the gravitational wave (gravity gradient) detector and laser guidance instrument are rarely affected by gas ionization. Both types of guidance systems work well and allow the HFVs to accurately identify/track targets even when the HFVs are at the highest speed in the final phase. In the cruise phase, our HFVs can also receive information from navigation satellites by laser communication to ensure the reliability of long-distance navigation under hypersonic conditions. The new method proposed by us is based on these researches, so actual HFVs have overcome the ionization black barrier through the composite guidance system when we designing controller.

IV. VERIFICATION EXPERIMENT

This section verifies the effectiveness of the designed variable structure NDI controller with active-passive hybrid compensation through experiments and result analysis.

After indoor simulation verification, we have performed HFV flight tests in three open spaces consisting of near-surface airspace over the East China Sea, Taiwan Strait and South China Sea. First, the normal variable structure flight is verified in the stratosphere above sea level and mildest climate without interference and uncertainty of inertia parameters (Section IV-A). Then the multi-mission profile flight mode such as high maneuvering and sea grazing flight is adopted near the sea, and the robustness of the proposed HFV controller is verified by using enemy interference and periodic wave and air disturbance in real battlefield environment. Finally, taking the real open space near the sea as the unified comparative test condition, the superiority of the proposed control scheme compared with the state-of-art method is also verified. Robustness and superiority verification are all in Section IV-B.

Table 2 displays the experiment conditions, with a data acquisition time of 20s. All experimental curves have small noise in the range of 10^{-4} of their respective physical units. This is the credit of the filter, but is not the focus of this study, we do not show the fine structure of the curves.

TABLE 2. HFV simulation condition parameters.

Parameter meaning	Symbol	Parameter value
HFV mass	m	9101.44kg
Pitch moment of inertia	I_y	65073.8kg·m^2
Reference wing area	S	27.03m^2
Maximum of variable structure parameter	ΔS_{max}	3.21m^2
Span	b	9.144m
Air density	ρ	1.312kg/m^3
Flight speed	V	7Ma
Track inclination angle	μ	0deg (°)

A. SIMULATION OF NOMINAL VARIABLE STRUCTURE NDI CONTROLLER

HFV normal coordinate overload *Nys* is expressed as

$$Nys=\frac{V}{g}(q-\dot{\alpha})+\frac{I_{xs}}{g}\dot{q} \tag{78}$$

The distance between the aircraft's center of gravity and the overload sensor is denoted by I_{xs}. The orbital inclination of HFV is expressed as

$$\mu=\theta-\alpha \tag{79}$$

Near an equilibrium point, the nonlinear variable structure HFV's linearization method must be employed, with the equilibrium state chosen as the angle of attack, $\alpha_0=3.25°$. Set the

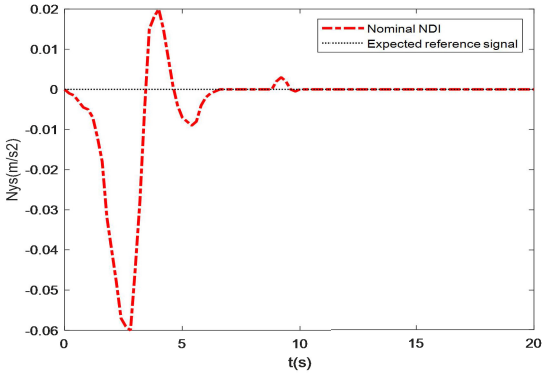

(a) Tracking curve of the normal overload *Nys*

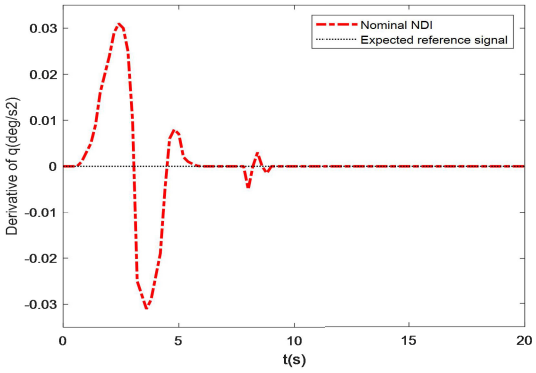

(b) Tracking curve of pitch rate derivative $\dot{q}$

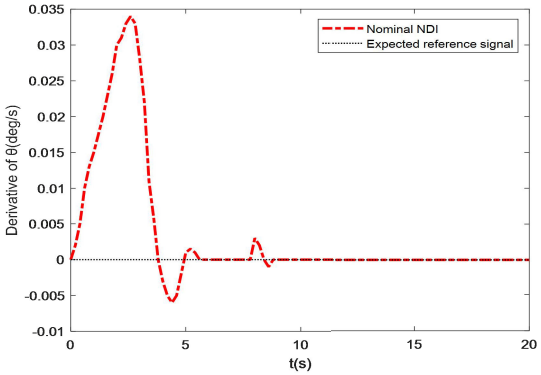

(c) Tracking curve of the pitch derivative $\dot{\theta}$

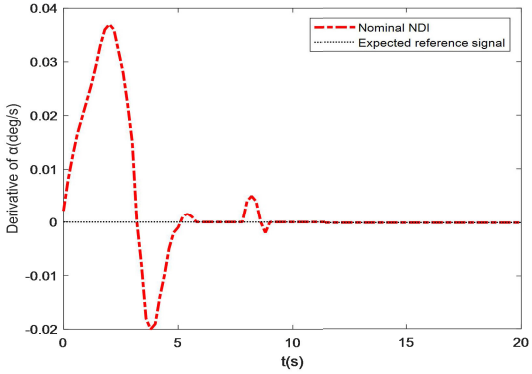

(d) Tracking curve of the attack angle derivative $\dot{\alpha}$

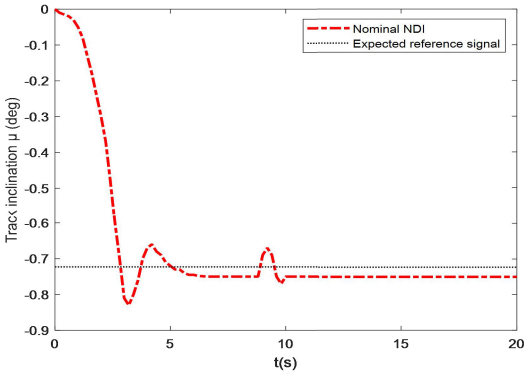

(e) Tracking curve of the track inclination μ

FIGURE 5. **Nominal variable structure NDI control under modeling error.**

reference signals to

$$\alpha_c = 4 \times \frac{\pi}{180}\text{rad}, q_c = 0\text{rad}/s, \theta_c = 3.27 \times \frac{\pi}{180}\text{rad},$$

The initial simulation conditions are $\alpha = 0$rad, $q = 0$rad/s, $\theta = 0$rad. The proportion coefficients of K and other variable structure harmonic functions are set as the following table.

TABLE 3. **Partial algorithm parameters.**

w_{11}	w_{22}	w_{33}	w_α	w_q	w_θ	k_1	k_2	k_3
3	10	6	0.7	25	0.2	104	69	80

HFV executes variable structure mode when $t = 8.5$s. Variable structure parameter is expressed as follows:

$$\Delta S = \begin{cases} 0, & t \in [0, 8.5) \\ 3.21 \tanh 1000(t - 8.5), & t \in [8.5, 20) \end{cases} \quad (80)$$

Part of the adaptive parameters of the model reference main loop are given in the proof, namely equation (48). Simulation results of nominal variable structure NDI controller are shown in Figure 5.

The simulation results show that the system model with modeling error can quickly return to the stable state under both fix structure and variable structure modes. The system state $x = [\alpha, q, \theta]^T$ can track the given reference command $x_c = [\alpha_c, q_c, \theta_c]^T$, the derivative of the state variable eventually tends to 0, and the normal overload *Nys* tends to 0, meeting the control objectives. Simulation results demonstrate that, when the system moves longitudinally, the default sideslip angle $\beta = 0$ and the chosen equilibrium state should guarantee the orbital inclination $\mu = 0$. Stability of μ is maintained at $-0.72°$ in both fixed and variable structure modes, yet the deviation is tolerable and stability remains unaffected. There is still room for improvement in compensating parametric uncertainty.

B. SIMULATION OF SLIDING MODE NDI WITH HYBRID ADAPTIVE COMPENSATION

This section continues the robustness and superiority verification based on the validity basic verification in the previous section. Under high-maneuver sea skimming flight condition, the uncertain inertia and disturbance are measured. Set the reference signals to

$$\begin{cases} \alpha_c = 4 \times \dfrac{\pi}{180}\text{rad} \\ q_c = 0\text{rad}/s \\ \theta_c = 3.27 \times \dfrac{\pi}{180}\text{rad}, \end{cases}$$

Uncertainty mainly affects the aerodynamic parameters M_z^{α}, $M_z^{\delta_e}$, $M_z^{\dot{\alpha}}$, and M_z^{q}. From the state matrices A, B, C, D of the system, it can be observed that these four aerodynamic parameters mainly affect the pitch rate channel and output $\dot{q}$, thus indirectly affecting the normal overload. The inertia uncertainty's effect is mainly seen in the changes of pitch angle and velocity. This uncertainty has been broadened to a range of $\pm 20\%$, with the pitching inertia I_y being:

$$I_y = I_{y0}(1 + \Delta I_y(2rand(1, 1) - 1)) \tag{81}$$

Observer (59) shows the ideal and estimation results of disturbance in Figure 6. The function vector is:

$$d(t) = [0.07\sin(t + 0.32) \quad 0.07\sin(t + 0.32) \times 0.07\sin(t + 0.32)]^T \tag{82}$$

Such disturbance simulate the periodic water and air resistance caused by periodic waves during sea skimming. The disturbance function represents the effect of wave interference on the signal, the function has no physical unit, and it will have unit after parameter matrix allocation.

A comparison of the simulation results of nominal variable structure NDI control and adaptive sliding mode NDI control with active-passive hybrid compensation is depicted in Figure 7, where the disturbance observer is denoted by 'DOB', for a longitudinal system with a moment of inertia uncertainty of $\pm 20\%$. The passive adaptive NDI to directly compensates the uncertainty of inertia and the active adaptive sliding mode NDI with observer compensates the disturbance.

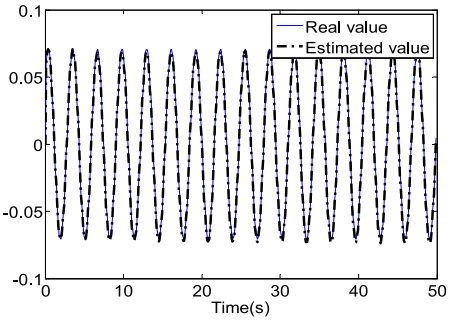

FIGURE 6. Disturbance curve and its estimation.

TABLE 4. Comparative analysis of performance indicators.

	State-of-art scheme in [26]	Nominal variable structure NDI	Adaptive sliding mode variable structure NDI
$t_{s,max}$	—	7.95	5.28
$t_{s,min}$	6.96	5.01	1.61
$e_{ss,max}$	∞	2.6	0.0004
$e_{ss,min}$	0.0003	0.0003	0.0001
$o_{v,max}$	—	30.39%	7.50%
$o_{v,min}$	16.65%	17.91%	0.03%

As shown in Figure 7, the sliding mode variable-structure NDI controller with hybrid compensation can reduce the oscillation of each channel when the HFV has an inertial uncertainty and disturbance. It can suppress the oscillation of the attitude angles and angular velocity better, especially in the variable structure mode; the nominal method has an apparent deviation, and the improved method maintains accurate tracking. This shows that the improved controller has stronger robustness to uncertainty and disturbance, and can pass the robustness test perfectly.

Table 4 lists the tracking performances based on the statistics shown in Figure 7. Based on the general definition of an overshoot, only Figure 7(e)∼(g) show the overshoot [29]. The three controllers in the table represent the variable-structure compensation of [26] and the two-variable-structure NDI in this study: the nominal, adaptive sliding mode with hybrid compensation.

The minimum response time ($t_{s,min}$) of the proposed hybrid compensation adaptive sliding mode controller is 32% of the nominal controller, the maximum steady-state error ($e_{ss,max}$) is 0.01% of the nominal controller, and the overturning ($o_{v,max}$) is 24% of the nominal controller. However, due to the divergent method in [26] under variable structure mode, the error is infinite, thus precluding the counting of

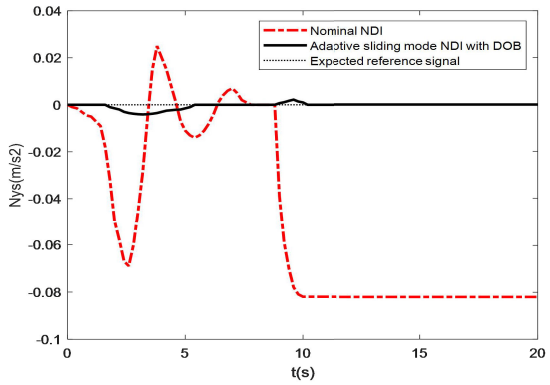

(a) Tracking curves of the normal overload *Nys*

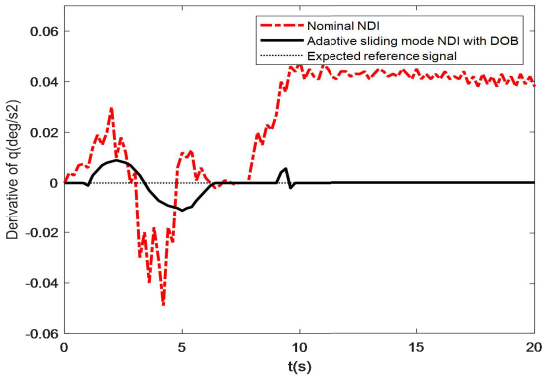

(b) Tracking curves of pitch rate derivative $\dot{q}$

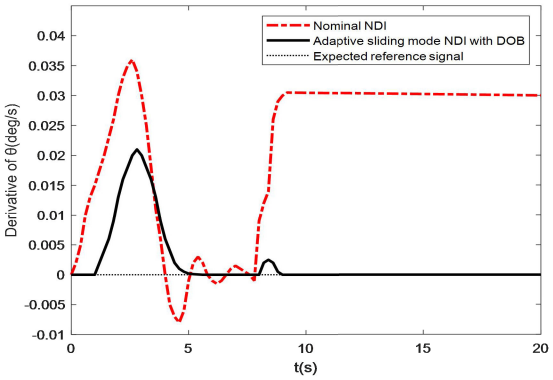

(c) Tracking curves of the pitch derivative $\dot{\theta}$

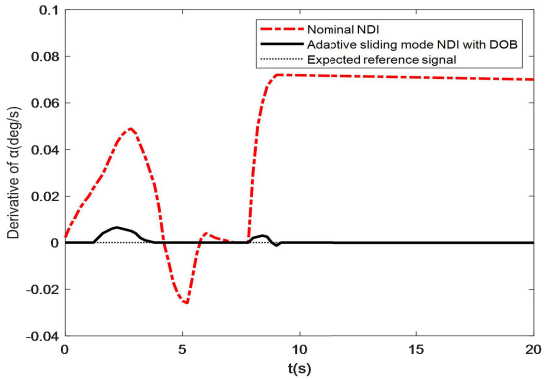

(d) Tracking curves of the attack angle derivative $\dot{\alpha}$

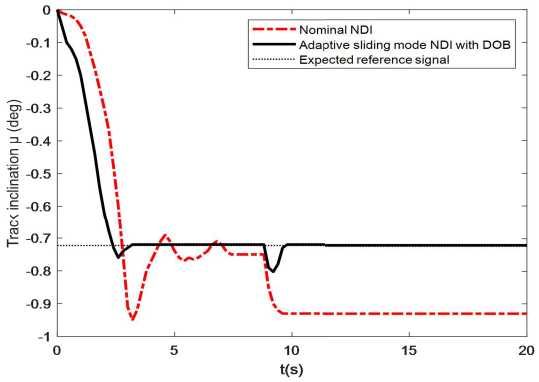

(e) Tracking curves of the track inclination μ

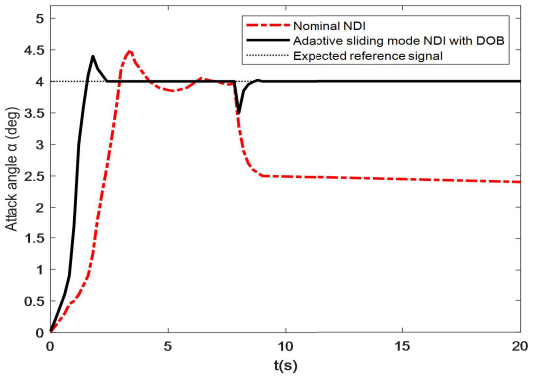

(f) Tracking curves of the attack angle α

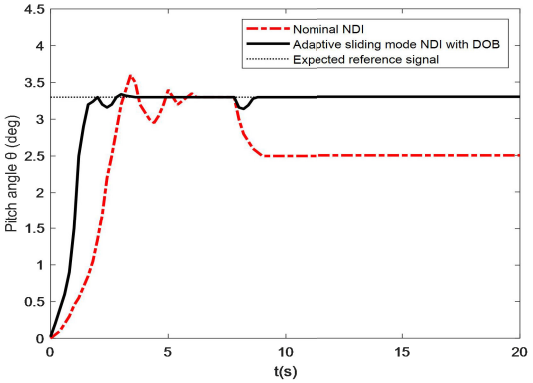

(g) Tracking curves of the pitch angle θ

FIGURE 7. **Comparison effects of different HFV controllers under inertia uncertainty and disturbance.**

maximum response time and overshoot (with no statistical data represented by '—'). A variable-structure NDI with an active-passive hybrid compensation function is suitable for high-manoeuvring sea-skimping HFV. This further shows the superiority of the proposed controller, which can be verified by the superiority test of the experimental setting.

V. CONCLUSION

In this study, the adaptive hybrid compensation method demonstrated can maintain the stability of variable structure HFV in the presence of multiple uncertainties. The nominal variable structure NDI controller compensates the modeling error. Thence the harmonic functions of self-adjusting with variable structure parameters successfully adapts to the non-variable structure mode and variable structure mode, ensuring the stability of the whole process of this kind of advanced HFV. Furthermore, the compound adaptive NDI controller successfully carries out direct passive compensa-tion for the inertial uncertainty by means of the multi-adaptive learning laws, which makes the variable structure HFV robust to the inertia uncertainty. In addition, the sliding mode disturbance observer not only realizes the accurate estimation of the sea skimming disturbance, but also helps the sliding mode variable structure NDI controller to actively repair the disturbance. Finally, the hybrid control strategy enables the variable structure HFV to obtain attitude stability by using passive-active compensations in the face of uncertain inertia and disturbance. The proposed method solves the multi-source uncertain robust control problem of variable structure HFV. The follow-up research will focus on the multi-fault automatic repair technology.

REFERENCES

[1] A. Abdelmawgoud, M. Jamshidi, and P. Benavidez, "Distributed estimation in multimissile cyber-physical systems with time delay," *IEEE Syst. J.*, vol. 14, no. 1, pp. 1491–1502, Mar. 2020.

[2] P. Gutiérrez León, J. García-Morales, R. F. Escobar-Jiménez, J. F. Gómez-Aguilar, G. López-López, and L. Torres, "Implementation of a fault tolerant system for the internal combustion engine's MAF sensor," *Measurement*, vol. 122, pp. 91–99, Jul. 2018.

[3] A. A. Amin and K. Mahmood-Ul-Hasan, "Advanced fault tolerant air-fuel ratio control of internal combustion gas engine for sensor and actuator faults," *IEEE Access*, vol. 7, pp. 17634–17643, 2019.

[4] Y. Yuan, X. Liu, S. Ding, and B. Pan, "Fault detection and location system for diagnosis of multiple faults in aeroengines," *IEEE Access*, vol. 5, pp. 17671–17677, 2017.

[5] F. Hao, D. Zhang, L. Cao, and S. Tang, "Disturbance decoupling control for flexible air-breathing hypersonic vehicles with mismatched condition," *Asian J. Control*, vol. 21, no. 3, pp. 1100–1110, May 2019.

[6] M. Zolfaghari, M. Abedi, and G. B. Gharehpetian, "Robust nonlinear state feedback control of bidirectional interlink power converters in grid-connected hybrid microgrids," *IEEE Syst. J.*, vol. 14, no. 1, pp. 1117–1124, Mar. 2020.

[7] H. Hassani, J. Zarei, R. Razavi-Far, and M. Saif, "Robust interval type-2 fuzzy observer for fault detection of networked control systems subject to immeasurable premise variables," *IEEE Syst. J.*, vol. 13, no. 3, pp. 2954–2965, Sep. 2019.

[8] N. Rong, Z. Wang, and H. Zhang, "Finite-time stabilization for discontinuous interconnected delayed systems via interval type-2 T–S fuzzy model approach," *IEEE Trans. Fuzzy Syst.*, vol. 27, no. 2, pp. 249–261, Feb. 2019.

[9] G. Yang, J. Yao, and N. Ullah, "Neuroadaptive control of saturated nonlinear systems with disturbance compensation," *ISA Trans.*, vol. 122, pp. 49–62, Mar. 2022.

[10] G. Yang, J. Yao, and Z. Dong, "Neuroadaptive learning algorithm for constrained nonlinear systems with disturbance rejection," *Int. J. Robust Nonlinear Control*, vol. 32, no. 10, pp. 6127–6147, Apr. 2022.

[11] Z. Guo, J. Guo, J. Zhou, and J. Chang, "Robust tracking for hypersonic reentry vehicles via disturbance estimation-triggered control," *IEEE Trans. Aerosp. Electron. Syst.*, vol. 56, no. 2, pp. 1279–1289, Apr. 2022.

[12] Y. Hu, Y. Geng, B. Wu, and D. Wang, "Model-free prescribed performance control for spacecraft attitude tracking," *IEEE Trans. Control Syst. Technol.*, vol. 29, no. 1, pp. 165–179, Jan. 2021.

[13] J. Sun, Z. Pu, J. Yi, and Z. Liu, "Fixed-time control with uncertainty and measurement noise suppression for hypersonic vehicles via augmented sliding mode observers," *IEEE Trans. Ind. Informat.*, vol. 16, no. 2, pp. 1192–1203, Feb. 2020.

[14] X. Y. Zhu and D. D. Li, "Robust fault estimation for a 3-DOF helicopter considering actuator saturation," *Mech. Syst. Signal Process.*, vol. 155, Jun. 2021, Art. no. 107624.

[15] X. Yang, W. Deng, and J. Yao, "Neural adaptive dynamic surface asymptotic tracking control of hydraulic manipulators with guaranteed transient performance," *IEEE Trans. Neural Netw. Learn. Syst.*, early access, Jan. 28, 2022, doi: 10.1109/TNNLS.2022.3141463.

[16] X. H. Chang and Y. Liu, "Robust H_∞ filtering for vehicle sideslip angle with quantization and data dropouts," *IEEE Trans. Veh. Technol.*, vol. 69, no. 10, pp. 10435–10445, Oct. 2020.

[17] L. Chen, Q. Wang, H. Ye, and G. He, "Low-complexity adaptive tracking control for unknown pure feedback nonlinear systems with multiple constraints," *IEEE Access*, vol. 7, pp. 27615–27627, 2019.

[18] F. Meng, K. Tian, and C. Wu, "Deep reinforcement learning-based radar network target assignment," *IEEE Sensors J.*, vol. 21, no. 14, pp. 16315–16327, Jul. 2021.

[19] H. An, J. Liu, C. Wang, and L. Wu, "Disturbance observer-based anti-windup control for air-breathing hypersonic vehicles," *IEEE Trans. Ind. Electron.*, vol. 63, no. 5, pp. 3038–3049, May 2016.

[20] X. Yu, P. Li, and Y. Zhang, "Fixed-time actuator fault accommodation applied to hypersonic gliding vehicles," *IEEE Trans. Autom. Sci. Eng.*, vol. 18, no. 3, pp. 1429–1440, Jul. 2021.

[21] K. Gao, J. Song, X. Wang, and H. Li, "Fractional-order proportional-integral-derivative linear active disturbance rejection control design and parameter optimization for hypersonic vehicles with actuator faults," *Tsinghua Sci. Technol.*, vol. 26, no. 1, pp. 9–23, Feb. 2021.

[22] A. A. Amin and K. M. Hasan, "A review of fault tolerant control systems: Advancements and applications," *Measurement*, vol. 143, pp. 58–68, Sep. 2019.

[23] K. Hu, C. Wen, and A. Yusup, "Improved adaptive hybrid compensation for compound faults of non-Gaussian stochastic systems," *IEEE Access*, vol. 7, pp. 51284–51294, 2019.

[24] G.-H. Yang and D. Ye, "Adaptive reliable H_∞ filtering against sensor failures," *IEEE Trans. Signal Process.*, vol. 55, no. 7, pp. 3161–3171, Jul. 2007.

[25] Y. Gao, F. Xiao, J. Liu, and R. Wang, "Distributed soft fault detection for interval type-2 fuzzy-model-based stochastic systems with wireless sensor networks," *IEEE Trans. Ind. Informat.*, vol. 15, no. 1, pp. 334–347, Jan. 2019.

[26] K. Y. Hu, W. H. Li, and Z. A. Cheng, "Fuzzy adaptive fault diagnosis and compensation for variable structure hypersonic vehicle with multiple faults," *PLoS ONE*, vol. 16, no. 8, pp. 1–20, Aug. 2021.

[27] K. Hu, F. Chen, and Z. Cheng, "Fuzzy adaptive hybrid compensation for compound faults of hypersonic flight vehicle," *Int. J. Control, Autom. Syst.*, vol. 19, no. 6, pp. 2269–2283, May 2021.

[28] A. Abratanski, R. Grzejda, and R. Perz, "Feasibility study of topology optimization of the control system frame for the missile with canard configuration," *Aircr. Eng. Aerosp. Technol.*, vol. 95, no. 5, pp. 814–819, Feb. 2023.

[29] B. Xiao, Q. Hu, D. Wang, and E. K. Poh, "Attitude tracking control of rigid spacecraft with actuator misalignment and fault," *IEEE Trans. Control Syst. Technol.*, vol. 21, no. 6, pp. 2360–2366, Nov. 2013.

[30] J. Su and W.-H. Chen, "Model-based fault diagnosis system verification using reachability analysis," *IEEE Trans. Syst., Man, Cybern., Syst.*, vol. 49, no. 4, pp. 742–751, Apr. 2019.

[31] M. K. Behera and L. C. Saikia, "An improved voltage and frequency control for islanded microgrid using BPF based droop control and optimal third harmonic injection PWM scheme," *IEEE Trans. Ind. Appl.*, vol. 58, no. 2, pp. 2483–2496, Mar. 2022.

[32] P. Ignaciuk and M. Morawski, "Quasi-soft variable structure control of discrete-time systems with input saturation," *IEEE Trans. Control Syst. Technol.*, vol. 27, no. 3, pp. 1244–1249, May 2019.
[33] A. Ghaffari and S. A. H. Dastja, "Safety-augmented operation of mobile robots using variable structure control," *IEEE Trans. Control Syst. Technol.*, vol. 30, no. 6, pp. 2751–2758, Nov. 2022.
[34] B. Tang, W. Lu, B. Yan, K. Lu, J. Feng, and L. Guo, "A novel position speed integrated sliding mode variable structure controller for position control of PMSM," *IEEE Trans. Ind. Electron.*, vol. 69, no. 12, pp. 12621–12631, Dec. 2022.
[35] Y. Ma, Z. Li, R. Malekian, R. Zhang, X. Song, and M. A. Sotelo, "Hierarchical fuzzy logic-based variable structure control for vehicles platooning," *IEEE Trans. Intell. Transp. Syst.*, vol. 20, no. 4, pp. 1329–1340, Apr. 2019.
[36] O. Bouyahia, F. Betin, and A. Yazidi, "Fault tolerant variable structure control of six-phase induction generator for wind turbines," *IEEE Trans. Energy Convers.*, vol. 37, no. 3, pp. 1579–1588, Sep. 2022.

KAI-YU HU received the Ph.D. degree from the Nanjing University of Aeronautics and Astronautics, Nanjing, China.

He was a Chief Designer with China State Shipbuilding Corporation. He is currently a Principal Engineer with China Aerospace Science and Industry Corporation. He has presided over the development of the world's largest airborne all-electric trailer and led the design of a fighter super-maneuverable controller. His current research interests include adaptive control, non-Gaussian systems, and self-repairing control.

YUQING CHENG received the master's degree in automation engineering from the School of Information Science and Engineering, Northeastern University, Shenyang, China, in 2022.

She is currently a Principal Engineer and the Technical Director of the Science and Technology Department, Beijing Jinghang Computation and Communication Institute (304th Institution), China Aerospace Science and Industry Corporation. Her research interests include adaptive control, flight control, quantum control, and self-repairing control.

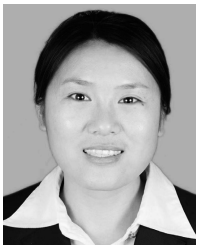

CHUNXIA YANG was born in Jining, Shandong. She received the Graduate degree from the University of Science and Technology Beijing, Beijing, China.

She is currently the Technical Director of the Science and Technology Department, Beijing Jinghang Computation and Communication Institute (304th Institution), China Aerospace Science and Industry Corporation. Her research interests include adaptive control, guaranteed performance control, and fault tolerant tracking control for hypersonic flight vehicle. She has extensive experience in software design.